measuring reactivity changes by the danger coefficient technique to within a few parts in 10^6. The fission product cross section transient due primarily to Xe^{135} and Sm^{149} was observed continuously from 1 hr to 60 hr after removal from the high flux region by observing the changes in the regulating rod position for criticality of the RMF. The reactor drift was eliminated by comparing the irradiated sample with an identical unirradiated sample every 30 min.

The regulating rod position changes were calibrated in terms of total capture cross section (number of atoms times σ capture) in the sample by a direct comparison with boron and U^{235} standards of known concentration. The standard samples duplicated the geometry and cross-section range of the irradiated samples to account for self-shielding. The data are obtained then as total poison capture cross section in cm^2 *versus* time after removal from the irradiating flux. A calculated value for the total Sm^{149} capture cross section *versus* time was then subtracted from the data giving net values of total capture cross section of Xe^{135} in cm^2 in the sample *versus* time. The Sm^{149} correction was about 1% of the maximum xenon value and almost negligible.

A total of 160 data points during the 60 hr was then fitted for least squares deviation to the known expression for the xenon transient after reactor shutdown. This gave the coefficients A and B in the following expression:

$$R(\text{cm}^2 \text{ xenon}) = Ae^{-\lambda_1 t} + Be^{-\lambda_2 t} \tag{1}$$

$$A = \frac{N\sigma_f\phi\sigma_2\gamma_1}{\lambda_2 - \lambda_1}, \quad B = \frac{(\gamma_1+\gamma_2)\sigma_2 N\sigma_f\phi}{\lambda_2+\sigma_2'\phi} - A,$$

where λ_1 = decay constant of I^{135} (0.1034 hr^{-1}), λ_2 = decay constant of Xe^{135} (0.0753 hr^{-1}), γ_1 = fission yield of Te^{135} and I^{135},‡ γ_2 = direct fission yield of Xe^{135}, σ_f = microscopic fission cross section of U^{235} (580 *b*),§ N = total U^{235} atoms in the fuel sample, ϕ = irradiating flux, σ_2 = microscopic capture cross section of Xe^{135}, σ_2' = microscopic capture cross section of Xe^{135} at irradiation temperature, and t = time after removal from irradiating flux.

Thus the product $\sigma_2\gamma_1$ may be extracted from the above equation as

$$\sigma_2\gamma_1 = A(\lambda_2 - \lambda_1)/(N\sigma_f\phi). \tag{2}$$

The coefficients A and B were obtained from the least squares fit to the data as

$$A = -4.97 \text{ cm}^2 \pm 1\% \quad \text{and} \quad B = 5.10 \text{ cm}^2 \pm 1\%.$$

The standard deviations of ±1% were determined from the multiple regression analysis.

The irradiating flux was measured from activation of a cobalt flux monitor inserted with the samples during the irradiation. The flux as measured with the cobalt monitor was corrected to give the effective fission flux as follows. In an independent irradiation a nearly identical sample of U^{235} was irradiated under similar conditions to approximately 25% U^{235} burnup, and the integrated flux measured with the cobalt monitor. The burnup of U^{235} and hence the number of fissions was accurately measurable in the RMF he after ttransients (Xe and Sm) had died out. Thus the flux as measured from cobalt activation could be corrected to give an effective flux for producing U^{235} fissions using the 580 *b* cross section. This correction decreased by 10% the flux as measured with cobalt. Since the irradiation for the transient measurement produced only 0.7% burnup, the U^{235} fissions could not be measured accurately with the RMF. However, the correction to the cobalt activation flux above is applicable and was used to give the true fissioning rate. Since the measured cross-section-yield product is inversely proportional to the flux, the flux value may be the dominant source of uncertainty. The corrected flux value as used is being more accurately determined by chemical analyses of the samples.

Inserting a corrected flux value of 1.40×10^{14} nv in Eq. (2) gives a value for the product of

$$\sigma_2\gamma_1 = 1.47\times10^{-19} \text{ cm}^2 \pm 5\%.$$

The cross section (σ_2) is at room temperature and represents the effective 2200-m/sec value for a 1/v absorber equivalent to xenon. This is based on the use of the 2200-m/sec value of boron (755 *b*) for the calibration of the RMF. The Maxwellian average at room temperature for the above product is obtained upon multiplying by $\pi^{\frac{1}{2}}/2$ giving $\sigma_2\gamma_1 = 1.30\times10^{-19}$ cm^2.

If a yield for I^{135} of 6.0%[3] is used, the Maxwellian average capture cross section of xenon at 300°K is calculated as 2.17×10^{-18} cm^2. The two values of the xenon capture cross section averaged over a Maxwellian thermal neutron flux distribution at 300°K reported by Bernstein and Smith[4] are 2.50 or 2.24×10^{-18} cm^2. Our result is in better agreement with the lower value. A complete paper will be published shortly describing the experimental detail, further analysis, and interpretation of the data.

The authors are indebted to the technical groups at the Materials Testing Reactor who assisted in these experiments. In particular, acknowledgment is owed Dr. E. Fast and the RMF group who operated the RMF and provided valuable assistance throughout this work. The authors are also indebted to Dr. W. F. Witzig of Bettis Atomic Power Division, Westinghouse Electric Corporation, for his assistance and advice in this work.

* Operated for the U. S. Atomic Energy Commission by Westinghouse under contract AT-11-1-GEN-14.

[1] G. R. Hopkins and M. R. Stuart, paper XXII-6, June, 1956 meeting, American Nuclear Society, Chicago, Illinois (unpublished).

† Operated for the U. S. Atomic Energy Commission by Phillips Petroleum Company at the National Reactor Testing Station, Idaho.

[2] Nyer, deBoisblanc, and Webster, Phillips Petroleum Company, Idaho Falls, Idaho, Report IDO-16108 (1953) (unpublished).

‡ The Te^{135} decays to I^{135} with a half-life of 2 min. For practical purposes, γ_1 may be considered as the effective yield of I^{135}.

§ The proper value depends on the manner of expressing the flux ϕ as described in this letter.

[3] E. P. Steinberg and L. E. Glendenin, Geneva Conference Paper No. 614 (June, 1955); Steinberg (private communication).

[4] S. Bernstein and E. C. Smith, *Progress in Nuclear Energy* (McGraw-Hill Book Company, Inc., New York, 1956), Vol. I, Chap. 5.

Effect of Magnetic Field on Coupled Helix Attenuators

M. H. Miller, B. Hershenov, and J. R. Black
Electrical Engineering Department, University of Michigan, Ann Arbor, Michigan

(Received June 15, 1957)

During the course of developing a coupled helix attenuator for use with a high-power traveling-wave tube, an interesting variation of the coupling as a function of magnetic field strength was observed. The experimental arrangement is illustrated by Fig. 1. A trifilar coupling helix wound from 0.002-in. Kanthal wire served the dual functions of a coupling mechanism and a lossy medium. Typical data describing the variation of attenuation as a function of axial magnetic field in the *S*-band frequency range is shown in Fig. 2.

The effect was observed to be bilateral and independent of the power level (one watt and lower) used in obtaining the data. Additional measurements were made on an isolated monofilar Kanthal helix using the same diameter wire. No change in attenuation of a microwave signal as a function of magnetic field was observed. In addition, no change in dc resistance of this helix as the magnetic field was varied was observed. A coupled helix

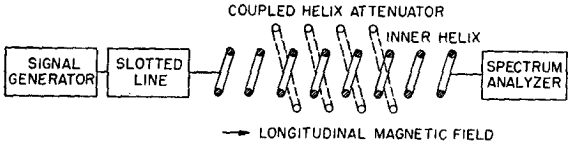

FIG. 1. Experimental arrangement for attenuation *vs* magnetic field measurements.

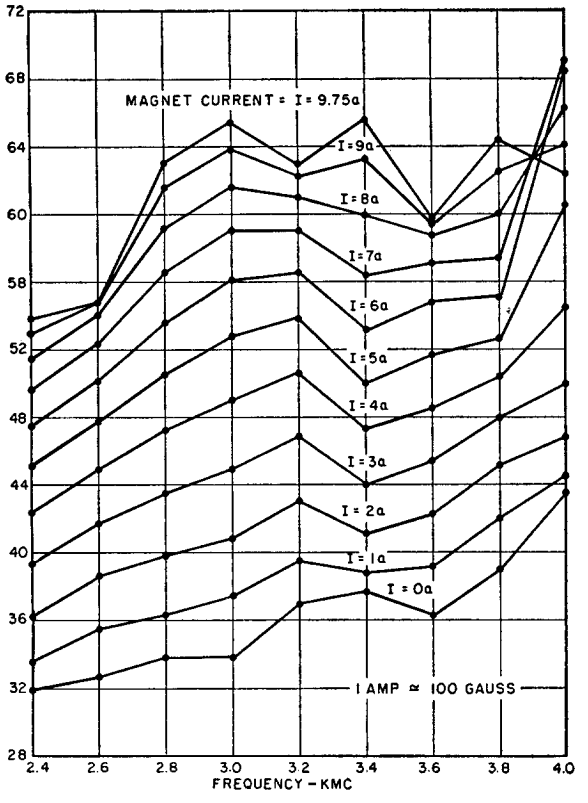

FIG. 2. Typical attenuation characteristics.

arrangement using 0.030-in. diameter Kanthal wire did not exhibit the effect. The change in attenuation with magnetic flux density is thought to be due to a variation of the coupling wavelength which, in turn, is due to a variation of the magnetic permeability of the Kanthal wire with applied magnetic field. Since the effect was not observed with larger diameter wires, it is believed to be associated with the crystalline directional properties of the fine wire resulting, possibly, from a drawing process during its manufacture.

It was also observed that a change in temperature yielded the same type of variation of attenuation. This characteristic was noted in the course of passing current through the coupling helix to provide a self-biasing magnetic field and a semiqualitative verification was made using the interior of a large electromagnet (having a large thermal time constant) as an oven.

Using a coupling helix which had been adjusted to deliver maximum attenuation in the center of the pass band, it was possible to shift the attenuation *vs* frequency characteristic with the magnetic field.

A novel application of this effect is its use as a stabilizing element in a traveling-wave tube to optimize operation at low- and high-power levels, respectively, by compensating for the five or six db gain difference between these two levels of operation. Other possible uses are as an electronically controllable attenuator and a low-frequency modulator.

Electrical Resistivity of Boron

E. S. GREINER AND J. A. GUTOWSKI
Bell Telephone Laboratories, Inc., Murray Hill, New Jersey
(Received July 29, 1957)

ELECTRICAL resistivity of polycrystalline boron has been measured at temperatures between −160 and 700°C on three specimens prepared by the reduction of boron trichloride with hydrogen on heated tungsten or tantalum filaments. Specimens *A* and *B* were deposited at 1380°C and specimen *C* was deposited at 1530°C.

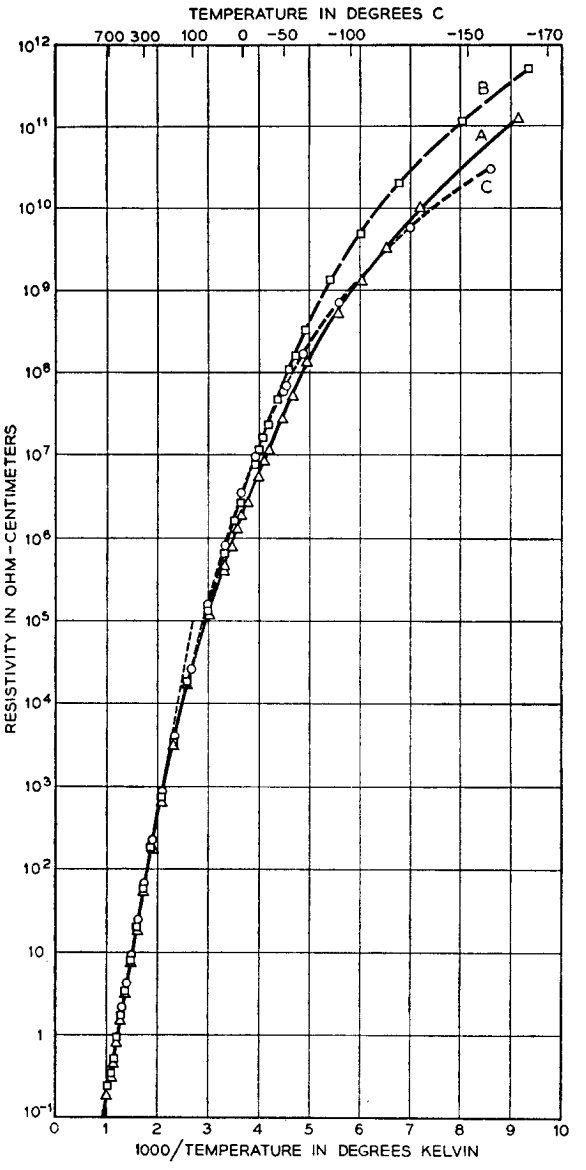

FIG. 1. Resistivity of three specimens of boron as a function of the reciprocal of the absolute temperature.

The specimens for electrical tests, separated from the tungsten or tantalum core, were about 0.3 cm long and 0.03 cm² in cross-sectional area. Platinum wires were fused to the ends of the specimens for electrical contacts. Resistivities at low temperatures were measured with a high impedance meter[1]; at high temperatures, the microammeter-potentiometer method was used. The thermocouples were calibrated to a precision of ±1°C. Resistances were measured to an accuracy of one percent, but owing to irregularities of the electrical contacts, the resistivities are accurate to five percent.

The values of electrical resistivity, Fig. 1, are in close agreement over the range measured. The differences in resistivity at low temperatures reflect variations in impurity content. Spectrochemical qualitative analysis revealed that specimens *A* and *B* contained not more than ~0.1% silicon and only slight traces or less (<0.005%) of a few other elements. Specimen *C*, the most